Korean J. Chem. Eng., **21**(4), 895-900 (2004)

An Electrochemical Study of Stainless Steels and a Nickel Alloy in a Decontamination Agent Using the Potentiodynamic Method

Hong-Joo Lee†, Duk-Won Kang* and Young Ju Lee**

Research Institute for Innovation in Sustainable Chemistry,
National Institute of Advanced Industrial Science and Technology (AIST), 1-1-1 Higashi, Tsukuba, Ibaraki 305-8565, Japan
*Nuclear Power Laboratory, Korea Electric Power Research Institute (KEPRI),
103-16 Munji-Dong, Yuseong-Gu, Daejeon 305-380, Korea
**Gwangju Branch, Korea Basic Science Institute (KBSI), 300 Yongbong-Dong, Buk-Gu, Gwangju 500-757, Korea
(*Received 23 September 2003 • accepted 19 April 2004*)

Abstract–Chemical decontamination is accepted as one of the effective methods for decreasing radioactivity from radioactive materials existing in the systems of the nuclear power plants. In chemical decontamination processes, metal oxides dissolve in chelating agents such as oxalic acid and EDTA (Ethylenediaminetetraacetic acid) in the dissolution step for the chemical decontamination process. It is important to investigate corrosion behaviors with respect to decontaminating agents in the development of decontamination process. In this study, the potentiodynamic method was considered among electrochemical methods in order to investigate corrosion behaviors of stainless steels (SS 316, SS 304) and a nickel alloy (Inconel 600). The corrosion behaviors observed in the potentiodynamic results agreed with those of corrosion behaviors observed in the weight loss method, showing that the electrochemical study is a very useful method for estimating corrosion behavior.

Key words: Corrosion, Electrochemical Method, Potentiodynamic Method, Decontaminating Agent

INTRODUCTION

Decontamination is generally accepted as an important means to eliminate or to lower radiation level of radioactive contaminants existing on the surfaces of buildings, equipment, components, system, etc., which are excessively exposed to radiation in nuclear power plants [Ocken, 1999; Wood et al., 1989; Varrin, 1996; Moon et al., 1997]. The decontamination methods can be classified into mechanical, electrical and chemical. Of methods, chemical decontamination is considered to be an effective method to dissolve cruds (radioactive corrosion products) and metal oxidizing films on the surface of tubes or systems using chemical decontaminating agents which consist of chemicals, such as chelating agents, reductants and oxidants [Ocken, 1999; Ayres, 1970; Lee et al., 2003].

In a previous study, a decontamination process using chemical decontamination agents was developed for the component decontamination in the primary systems of Korean pressurized water reactors (PWR) [Kim et al., 2003a]. The chemical decontamination process consists of four steps, including oxidation, reduction, dissolution and decomposition/cleanup steps [Kim et al., 2004]. The schematic diagram of the decontamination process is shown in Fig. 1. Of four consecutive steps, metal oxides consisting of Fe, Cr, Ni as major components and Co as a minor component are dissolved into the solution containing chelating agents such as oxalic acid and EDTA (Ethylenediaminetetraacetic acid) in the dissolution step [Hur et al., 2003; Bayri et al., 1996]. Therefore, the dissolution step is considered to be the most important one to determine the decontamination effectiveness in the chemical decontamination process.

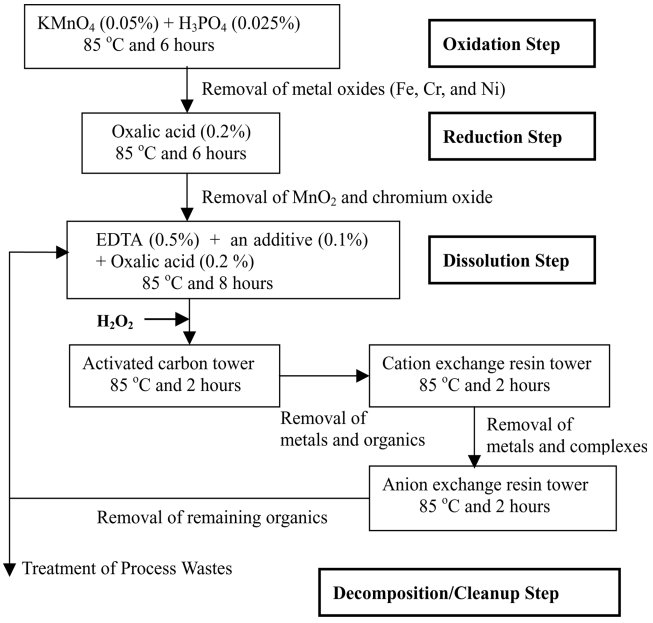

Fig. 1. Flow diagram for the chemical decontamination process.

It is important to select decontaminating agents having less corrosive effect on base materials as well as high decontamination efficiency for the development of decontamination processes [Varga et al., 2001; Yang et al., 1996; Dubourg, 1995]. In addition, a proper method should be considered to estimate the effects of the decontaminating agents on the corrosion with respect to base materials in a rapid and exact manner. The weight loss method measuring weight difference of testing coupons between before and after decontami-

†To whom correspondence should be addressed.
E-mail: hj-lee@aist.go.jp

nation experiments is accepted as one of the fundamental methods for evaluating corrosion rates on the base materials. This technique is considered to be the most satisfactory method of making a preliminary selection to observe different corrosion behaviors. However, it has difficulty in determining localized corrosion and in estimating corrosion rate in a short time [Fontata, 1987]. As a complementary method for corrosion behavior estimation, electrochemical methods are finding increasing practical applications of corrosion studies. The electrochemical methods provide a better understanding of the basic mechanisms and kinetics of the electrochemical reactions, which are related to the corrosion behavior of different material/electrolyte combinations, the availability of improved electrochemical techniques for the study of corrosion phenomena, and the demonstration of corrosion monitoring and control [Bard and Faulkner, 1980; Rout et al., 2003; Kim et al., 2000; Park et al., 2003].

Of electrochemical methods to measure corrosion rates of base materials, the potentiodynamic method is one of the commonly considered methods in corrosion studies [Sedriks, 1990; Siebert, 1985]. The increase of potentials during the potentiodynamic measurements causes a corrosion cell to produce electrical currents, which are recorded in a computer file together with the applied potentials. During the potentiodynamic measurements, both potentials and currents are plotted in a polarization curve to allow for the observation of corrosion behaviors using the Tafel extrapolation technique [Tong, 1984; Lin et al., 2002; Veawab et al., 2001].

In order to investigate corrosion behaviors with respect to the chemical decontaminating agents by using the potentiodynamic method, a nickel alloy (Inconel 600) and a stainless steel (SS 304) were selected as testing materials for the laboratory decontamination experiments because they are base materials for a steam generator and tubes in the primary systems of PWR, respectively. In addition, SS 316 was considered as a reference material to compare corrosion effects in the environment of chemical decontaminating agents (see Table 1). And the results for the different corrosion behaviors were compared with those of the weight loss method in the semi-pilot scale decontamination experiments.

Table 1. Compositions of major materials existing in the primary systems of PWR

Base material		Steam generator	Tube	Reference
		Inconel 600	SS 304	SS 316
Relative composition (%)	Fe	8.0	65-70 (Balance)	65-70 (Balance)
	Ni	72.0 min (Balance)	8-10.5	10-14
	Cr	15.5	18-20	16-18
	Mn	1.0 max	2.0 max	2.0 max
	C	0.065	0.08 max	0.8 max
	S	0.015 max	0.03 max	0.03 max
	Si	0.5 max	1.00 max	1.00 max
	P	0.015 max	0.045 max	0.045 max
	Cu	0.5 max	-	-
	Mo	-	-	2-3
Density (g/cm^3)		8.45	8.00	8.00
Contacting area to coolant		75%	5%	-

EXPERIMENTAL

The 3-electrode electrochemical cell of a cylindrical type consists of saturated calomel electrode (SCE) in a Luggin capillary tube as a reference electrode and a platinum plate as a counter electrode, which is connected to the electrochemical system, Autolab 30 Potentiostat/Galvanostat (Electrochime, The Netherlands) [Choi et al., 2001]. In order to investigate different corrosion rates, stainless steels (SS 304, SS 316) and a nickel alloy (Inconel 600) were used as working electrodes having an effective area of 5 cm^2. The scan rates were varied from 0.17 mV/s to 68 mV/s in order to investigate scan rate effects on the corrosion potentials and currents. The solution temperatures were changed between 18 °C and 80 °C. The solution for the electrochemical methods was prepared with 3.6 mM NaFeEDTA (Aldrich, USA) in 0.5% Na_2EDTA (Aldrich, USA) as synthetic complex of metal/chelating agent. The chemical species and concentrations in the study were determined from those of the dissolution step, where the metal complexes of EDTA formed as results of metal oxide dissolution [Kim et al., 2003a]. Through measurement of potentials and corresponding currents the solution pH values were measured at 3.2±0.3 without pH control.

RESULTS AND DISCUSSION

1. Effects of Temperature on the Potentiodynamic Measurements

Potentiodynamic polarization measurement of metals and alloys indicates the tendency of a metal to undergo active, passive and transpassive behaviors [Ateya et al., 2002; Omanovic and Roscoe, 1999; Kim et al., 2003b]. At the active region in the neutral environment, the following reaction occurs in the solution as follows:

$$2H_2O+2e^- \rightarrow H_2+2OH^-. \quad (1a)$$

Under an acidic condition in these experiments, the occurring reduction reaction is as follows:

$$2H^++2e^- \rightarrow H_2. \quad (1b)$$

The reaction for the hydrogen production is monitored with relationship between potential and corresponding current. Fig. 2 shows

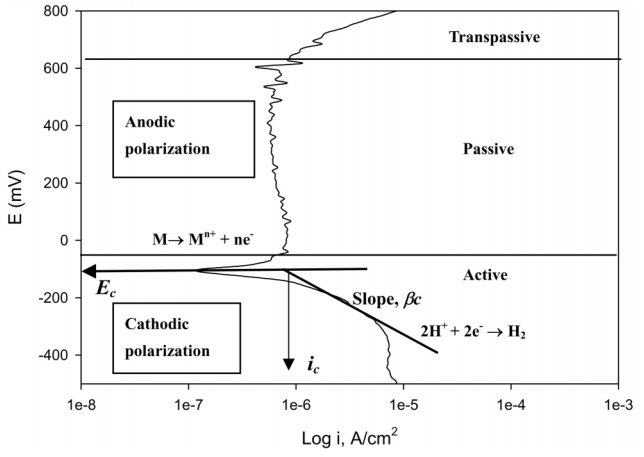

Fig. 2. Typical potentiodynamic polarization curve showing active, passive and transpassive regions.

the typical electrochemical polarization curve for SS 316 in the acidic solution. Considering the reactions on the working electrodes, the dissolution of metals takes place, *i.e.*:

$$M \rightarrow M^{n+} + n\,e^{-}. \quad (2)$$

In the typical cathodic polarization data for different materials in the acidic condition, the intersection between extrapolation of the cathodic Tafel slope (β_c) and the corrosion potential (E_c) gives the corrosion current density (i_c). The corrosion current density is calculated by using the following equation in the cathodic and anodic polarization curves, *i.e.*:

$$i_c = \frac{1}{2.3}\frac{i_{app}}{\Delta\phi}\left(\frac{\beta_c\beta_a}{\beta_c+\beta_a}\right) \quad (3)$$

where, i_{app} is the applied current density, $\Delta\phi$ the polarization potential value, and β_c and β_a the Tafel slopes of the cathodic and anodic reactions, respectively. In general, the experimental anodic polarization curves do not correspond to the idealization, showing no sensible linearity of the values of the anodic Tafel slope (β_a). It is suggested that anodic dissolution of metal is reversible in corroding solutions in the anodic polarization region [Fontata, 1987; Jones, 1996; Kim et al., 2003b].

In order to investigate the effect of temperature on the potentiodynamic measurements, the solution temperatures were varied from 18 °C to 80 °C at the scan rate of 3.4 mV/s. As shown in Fig. 3, the corrosion potentials of SS 304 and Inconel 600 slightly increased with increasing temperature, suggesting that the passivities of the metals decreased due to the solution containing EDTA. Meanwhile, the corrosion potentials of SS 316 showed similar values even with increasing temperatures. In addition, the Tafel constants with increasing temperatures for stainless steels and a nickel alloy were estimated and the results were shown in Fig. 4. In the investigation of the temperature effects on the Tafel constants, SS 316 showed similar values (between −560 mV and −583 mV), indicating that increasing solution temperatures gave little corrosion effect. However, it was observed that the corrosion behaviors were affected with increasing solution temperatures for SS 304 and Inconel 600.

The dependence of the rate of a metal dissolution process on temperature can be explained by using an Arrhenius type equation:

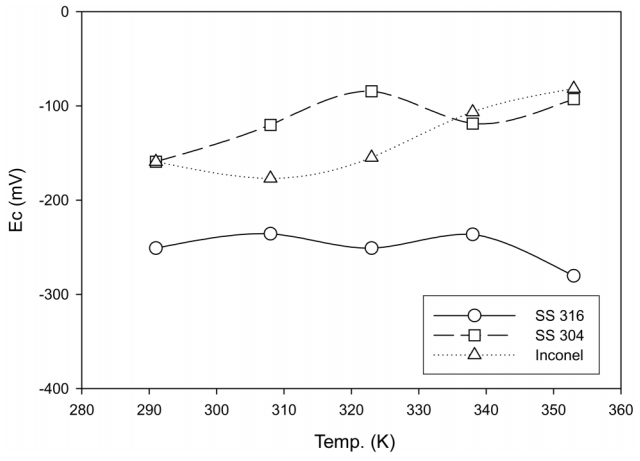

Fig. 3. Temperature effects on the corrosion potential (E_c) with different base materials.

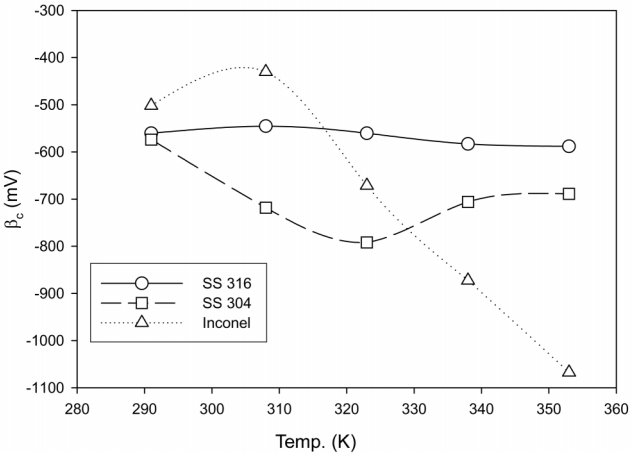

Fig. 4. Temperature effects on the Tafel constant (β_c) with different base materials.

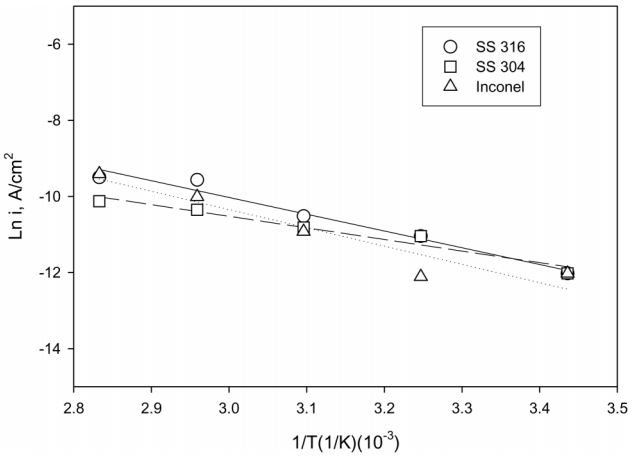

Fig. 5. Estimation of activation energies with different base materials.

$$i_c = Ae^{-E_a/RT} \quad (5)$$

where i_c (A/cm^2) is the corrosion current, E_a (J/mol) is the activation energy of corrosion, and A is a pre-exponential factor [Omanovic and Roscoe, 1999]. An Arrhenius plot of the corrosion currents for SS 304 in Fig. 5 shows stronger effect on the solution temperatures. The slope in the figure was estimated as −3.046, the least value among tested materials. The calculated result for the activation energy was found to be 25.3 KJ/mol. The results for SS 316 and Inconel 600 represented straight lines with the slope of −4.397 and −4.799, respectively. The activation energies from the slopes of the lines in Eq. (5) were 36.5 KJ/mol for SS 316 and 39.8 KJ/mol for Inconel 600. It is well known that temperature has a profound influence on the coefficients and diffusion rates, which is also explained by an Arrhenius type equation:

$$D = D_0 e^{-E_a/RT} \quad (6)$$

where D is the diffusion coefficient and D_0 is the temperature-independent pre-exponential coefficient. Eq. (6) means that the least activation energy results in the highest diffusion coefficient [Omanovic and Roscoe, 1999]. Therefore, the least value of the activa-

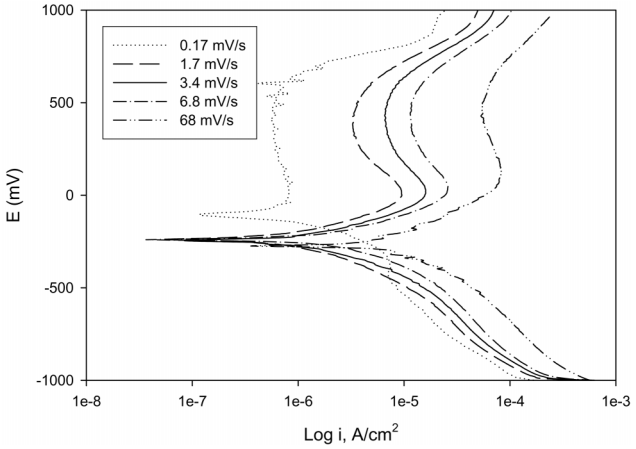

Fig. 6. Potentiodynamic behaviors of SS 316 with increasing scan rates.

tion energy for SS 304 implies the highest value of diffusion coefficients in the solution containing metal complex of EDTA.

2. Effect of Scan Rate on the Potentiodynamic Measurements

Fig. 6 shows the potentiodynamic measurement results of SS 316 with increasing scan rates from 0.17 to 68 mV/s (about 400-fold). As the values of scan rates increased, the current values increased both in the cathodic and anodic polarization regions. The variation of the current shown in the passive region of the anodic polarization clearly presented electron transfer during electrochemical measurements of the slowest scan rate (0.17 mV/s) [Siebert, 1985; Tong, 1984]. Meanwhile, the potentiodynamic polarization plots at the higher values of the scan rates showed smooth curves compared with the graph for the scan rate of 0.17 mV/s. It is assumed that the effects of the electron transfer on the polarization curves were affected by the scan rate in the potentiodynamic measurements.

Table 2 summarizes the results of the influences of scan rate on the electrochemical properties, such as the Tafel constant (β_c), corrosion potential (E_c), and corrosion current (i_c). Considering the corrosion potential of the cathodic polarization of stainless steels (SS 304 and SS 316) and a nickel alloy (Inconel 600), the corrosion potential of SS 316 showed the lowest value as −114 mV, while those of SS 304 and Inconel 600 showed the similar values with −56 mV and −55 mV. The transition from the passive region to the transpassive one occurred around at 629 mV. It was found that corrosion potentials reduced or became more negative at low scan rates. However, all the scan rates (above 1.7 mV/s or higher) showed similar values as shown in the figure. Meanwhile, the corrosion potentials of the nickel alloy clearly decreased down to −442 mV as the scan rates increased. In addition, the Tafel constant (β_c) in the cathodic polarization region decreased at low scan rates (up to 3.4 mV/s) and then showed similar values, irrespective of different base materials. Since the Tafel constant is related to the hydrogen production, the increasing scan rates of potential decreased hydrogen production during potentiodynamic measurements [Kim et al., 2003b]. As the scan rates increased, the corrosion currents for the anodic dissolution in the active region increased.

In the relationship between scan rate and corresponding current, it is known that the electrochemical system is diffusion-controlled when the resulting current is proportional to the square root of scan rate [Bard and Faulkner, 1980]. Fig. 7 clearly shows that corrosion currents increased proportionally according to the square root of the potential scan rates, suggesting that the rate of the charge transfer in the system is mainly affected by diffusion. The slope of SS 316 in the figure showed the lowest value as 2.21. In addition, the values of the linear slope in the plot of the root of scan rates and i_c for SS 304 and Inconel 600 were 2.93 and 4.92, respectively. The highest value for the Inconel 600 implies that corrosion rates largely increased with increasing potential scan rates. The results indicate that the rate-determining step of the anodic dissolution reaction in-

Table 2. Electrochemical parameters for SS 316, SS 304 and Inconel 600 in the potentiodynamic measurements

(a) SS 316

Scan rate (mV/s)	β_c (mV)	E_c (mV)	i_c (μA/cm^2)
0.17	−314	−114	1.3
1.7	−545	−236	3.0
3.4	−560	−251	6.0
6.8	−583	−236	9.0
68	−565	−280	19.0

(b) SS 304

Scan rate (mV/s)	β_c (mV)	E_c (mV)	i_c (μA/cm^2)
0.17	−188	−56	1.4
1.7	−501	−118	6.1
3.4	−573	−159	6.0
6.8	−541	−190	6.7
68	−592	−274	25.0

(c) Inconel 600

Scan rate (mV/s)	β_c (mV)	E_c (mV)	i_c (μA/cm^2)
0.17	−452	−55	3.5
1.7	−480	−138	5.1
3.4	−502	−159	6.0
6.8	−553	−190	7.8
68	−516	−442	40.0

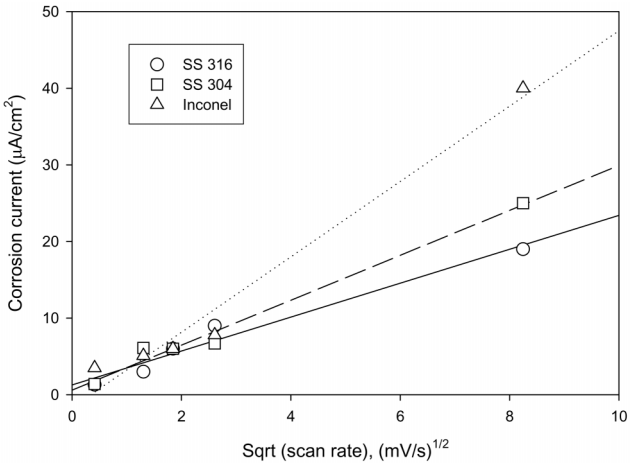

Fig. 7. Relationship between square roots of scan rate and corresponding corrosion current.

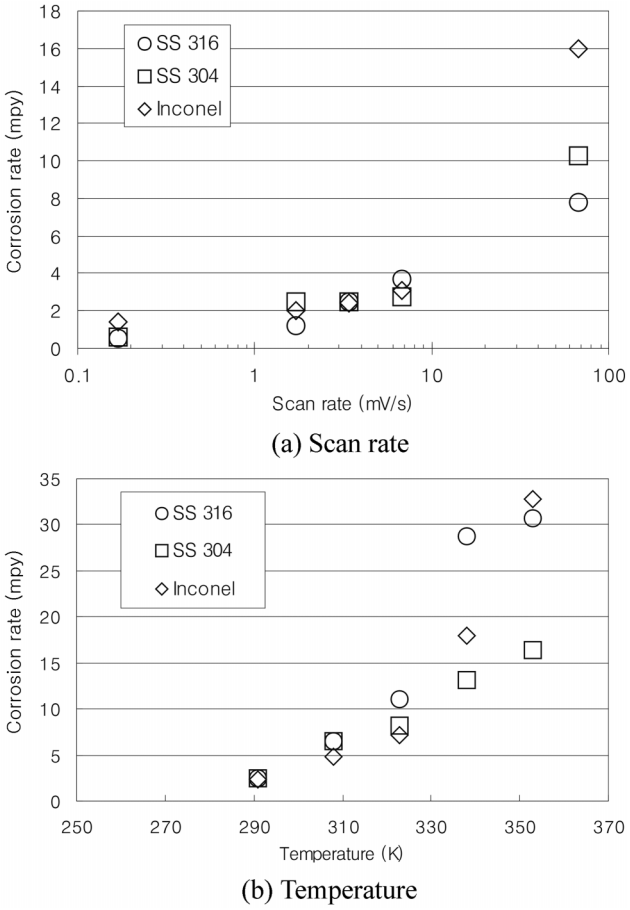

Fig. 8. Estimation of the corrosion rates of base materials with scan rates and temperature.

volves diffusion of reactant species in the electrolyte.

3. Estimation of Corrosion Rates in the Potentiodynamic Method

The corrosion rate in the electrochemical method can be estimated by the corrosion current density using Eq. (4):

$$r = 0.129\frac{ai_c}{nD} \quad (4)$$

where r is the corrosion rate expressed as mpy (mils per year), a atomic weight, n the number of electrons transferred, D the density (g/cm^3), i_c the corrosion density ($\mu A/cm^2$). It is considered that the resulting values of the corrosion rates are useful to estimate corrosion behaviors even though they show higher values compared with the results of the weight loss method [Jones, 1996].

In order to compare the corrosion behavior, the corrosion rates were estimated based on the corrosion currents, and expressed as mpy (mils per year) [Jones, 1996]. Fig. 8 illustrates the corrosion rates with increasing scan rates and temperatures. In the ranges of scan rate up to 6.8 mV/s, the corrosion rates showed low values, about below 4 mpy. The highest scan rate of 68 mV/s, however, presented significantly high values for all base materials. The scan rate effects on the corrosion rate were different with different base materials. Of base materials, the nickel alloy, Inconel 600, presented the highest value among tested materials. Also, the corrosion rates increased with increasing temperature for all base materials.

Based on the results of the semi-pilot scale experiments, the corrosion rates for SS 316, SS 304 and Inconel 600 were estimated by using the weight loss method after the oxidation and the dissolution processes. The results showed that Inconel 600 had somewhat higher values than stainless steels (SS 304 and SS 316) (See Table 3). Of materials, SS 304 showed the least corrosion rate of the planar specimens with the range of $0.63\text{-}0.93\times10^{-3}$ mg/cm^2 hr (0.012-0.017 mpy) and the average value of 0.77×10^{-3} mg/cm^2 hr (0.014 mpy). It is interesting that a nickel alloy, Inconel 600, showed the highest corrosion rate with the range of $2.30\text{-}4.04\times10^{-3}$ mg/cm^2 hr (0.039-0.069 mpy). Still, the corrosion rates of the stainless steel and the nickel alloy are considered acceptably low compared with the reference values for the corrosion behaviors [Jones, 1996].

The estimated corrosion rates of the potentiodynamic measurements at the experimental conditions of 80 °C and 3.4 mV/s were much higher than those of the weight loss measurements. It is likely that the experimental conditions in the potentiodynamic measurements were more severe compared with decontamination experimental conditions. Despite the high values of the results, the corrosion behaviors of different base materials were similar to those of the weight loss method. It is considered, through the electrochemical studies, that the potentiodynamic method is a very useful electrochemical method for estimating corrosion behaviors in a short time.

CONCLUSIONS

Electrochemical methods were used in a solution containing metal complex with EDTA in order to investigate corrosion behaviors of stainless steels (SS 316, SS 304) and a nickel alloy (Inconel 600) during chemical decontamination process. Of base materials, the nickel alloy, Inconel 600, presented the highest value of the corrosion current among tested materials. Also, the corrosion currents increased with increasing temperature and scan rates for all base

Table 3. Estimation of the corrosion rates of materials in the potentiodynamic methods and the weight loss measurements

	Potentiodynamic method (3.4 mV/s, 80 °C)	Weight loss method[a]					
		Minimum		Maximum		Average	
	mpy	($\times10^{-3}$) mg/cm^2 h	mpy	($\times10^{-3}$) mg/cm^2 h	mpy	($\times10^{-3}$) mg/cm^2 h	mpy
SS 304	16.4	0.63	0.012	0.91	0.017	0.77	0.014
SS 316	30.8	1.26	0.023	1.32	0.024	1.29	0.023
Inconel 600	32.8	2.30	0.039	4.04	0.069	3.17	0.054

[a]Data were referred from the reference [Kim et al., 2004].

materials. The corrosion behaviors observed in the potentiodynamic results agreed with those of corrosion behaviors observed in the weight loss method. It is considered that the estimated corrosion rates of the stainless steel and the nickel alloy were acceptably low. It was clearly confirmed that the potentiodynamic results corresponded to the results of the weight loss measurement, implying that the electrochemical method is a very useful method to estimate corrosion behaviors.

REFERENCES

Ateya, B. G., Al Kharafi, F. M. and Abdalla, R. M., "Electrochemical Behavior of Low Carbon Steel in Slightly Acidic Brines," *Materials Chemistry and Physics*, **78**, 534 (2002).

Ayres, J. A., "Decontamination of Nuclear Reactors and Equipment," Ronald Press, New York (1970).

Bard, A. J. and Faulkner, L. R., "Electrochemical Methods-Fundamentals and Applications," John Wiley & Sons (1980).

Bayri, B., Rosset, R., Desbarres, J., Jardy, A., Noel, D., Kerrec, O. and Lantes, B., "Complexing Properties of the Main Organic Acids Used in Decontamination Solutions for Nuclear Power Plants and Reactions Involved in Their Degradation or Elimination," *Nucl. Eng. Des.*, **160**, 159 (1996).

Choi, J. H., Lee, H. J. and Moon, S. H., "Effects of Electrolytes on the Transport Phenomena in a Cation-Exchange Membrane," *J. Colloid Interf. Sci.*, **238**, 188 (2001).

Dubourg, M., "Hard Chemical Decontamination of Steam Generator Tube Bundles," *Nucl. Eng. Des.*, **159**, 123 (1995).

Fontata, M. G., "Corrosion Engineering," 3rd ed., McGraw-Hill (1987).

Hur, D. H., Choi, M. S., Kim, U. C. and Han, J. H., "Magnetite Dissolution and Corrosion Behavior in High Temperature EDTA Solvents," *Nucl. Eng. Des.*, **220**, 11 (2003).

Jones, D. A., "Principles and Prevention of Corrosion," 2nd ed., Prentice Hall (1996).

Kim, K., Lee, H. J., Kang, D. W. and Inoue, S., "Synthesis of Simulated Cruds for Development of Decontaminating Agents," *Nucl. Eng. Des.*, **223**, 329 (2003a).

Kim, K., Lee, H. J., Choi, M., Kang, D. W. and Inoue, S., "Establishment of an Optimal Decontamination Process on a Newly Designed Semi-Pilot Equipment," *Nucl. Eng. Des.*, **229**, 91 (2004).

Kim, S. J., Okido, M. and Moon, K. M., "An Electrochemical Studies of Cathodic Protection of Steel Used for Marine Structures," *Korean J. Chem. Eng.*, **20**(3), 560 (2003b).

Kim, Y. S., Mitton, D. B. and Latanision, R. M., "Corrosion Resistance of Stainless Steels in Chloride Containing Supercritical Water Oxidation System," *Korean J. Chem. Eng.*, **17**(1), 58 (2000).

Lee, H. J., Kang, D. W., Chi, J. and Lee, D. H., "Degradation Kinetics of Recalcitrant Organic Compounds in a Decontamination Process with UV/H_2O_2 and $UV/H_2O_2/TiO_2$ Processes," *Korean J. Chem. Eng.*, **20**(3), 503 (2003).

Lin, H. C., Lin, K. M., Lin, C. S. and Ouyang, T. M., "The Corrosion Behaviors of Fe-based Shape Memory Alloys," *Corrosion Science*, **44**, 2013 (2002).

Moon, J. K., Byun, K. H., Park, S. Y. and Oh, W. Z., "Dynamic Simulation of Cyclic Voltammogram on the Electrochemical Reduction of VO^{2+} Ions," *Korean J. Chem. Eng.*, **14**(6), 521 (1997).

Ocken, H., "Decontamination Handbook," EPRI Report TR-112352 (1999).

Omanovic, S. and Roscoe, S. G., "Electrochemical Studies of the Adsorption Behavior of Bovine Serum Albumin on Stainless Steel," *Langmuir*, **15**, 8315 (1999).

Park, K. S., Cho, M. H., Park, S. H., Sun, Y. K., Lee, Y. S., Yoshida, M. and Nahm, K. S., "Optimization of $LiNiO_2$ Synthetic Condition and Effect of Excess Lithium and Al Doping on Electrochemical Characteristics of the Lithium Nickel Oxides," *Korean Chem. Eng. Res.*, **41**(1), 68 (2003).

Rout, T. K., Jha, G., Singh, A. K., Bandyopadhyay N. and Mohanty, O. N., "Development of Conducting Polyaniline Coating: a Novel Approach to Superior Corrosion Resistance," *Surface of Coatings Technology*, **167**, 16 (2003).

Sedriks, A. J., "Stress Corrosion Cracking Test Methods," NACE (National Association of Corrosion Engineers) (1990).

Siebert, O. W., "Laboratory Electrochemical Test Methods. Laboratory Corrosion Tests and Standards," ASTM STP 866, Haynes, G. S. and Baboian, R., eds., American Society for Testing and Materials (ASTM), Philadelphia (1985).

Tong, H. S., "Corrosion and Electrochemical Behavior of Iron-Chromium-Nickel Alloys in Concentrated Sulfuric Acid Solutions, Electrochemical Corrosion Testing," ASTM STP 727, Mansfield, F. and Bertocci, U., eds., American Society for Testing and Materials, Philadelphia (1984).

Varga, K., Hirschberg, G., Nemeth, Z., Myburg, G., Schunk, J. and Tilky, P., "Accumulation of Radioactive Corrosion Products on Steel Surfaces of VVER-Type Nuclear Reactors, II. ^{60}Co," *J. Nucl. Mat.*, **298**, 231 (2001).

Varrin, R. Jr., "Characterization of PWR Steam Generator Deposits," EPRI Report TR-106048 (1996).

Veawab, A. V., Tontiwachwuthikul, P. and Chakma, A., "Investigation of Low-Toxic Corrosion Inhibitors for CO_2 Separation Process Using Aqueous MEA Solvent," *Ind. Eng. Chem. Res.*, **40**, 4771 (2001).

Wood, C. J. and Spalaris, C. N., "Sourcebook for Chemical Decontamination of Nuclear Power Plants," EPRI Special Report NP-6433 (1989).

Yang, I. J., Teng, M. Y., Huan, W. I. and Sun, Y. L., "Decontamination of the Reactor Coolant in Maanshan Nuclear Power Plant," *Nucl. Eng. Des.*, **167**, 91 (1996).